Theor Appl Climatol (2016) 123:161–170
DOI 10.1007/s00704-014-1347-0

ORIGINAL PAPER

Time irreversibility of mean temperature anomaly variations over China

Fenghua Xie · Zuntao Fu · Lin Piao · Jiangyu Mao

Received: 21 April 2014 / Accepted: 11 December 2014 / Published online: 28 December 2014

Abstract Time-irreversible symmetry is a fundamental property of nonlinear time series. Time-irreversible behaviors of mean temperature measured on 182 stations over China from 1960 to 2012 are analyzed by directed horizontal visibility graph (DHVG for short), and significance of results has been estimated by Monte Carlo simulations. It is found that dominated time irreversibility emerges in nearly all daily temperature anomaly variations over China. Further studies indicate that these time-irreversible behaviors result from asymmetric distributions of persistent daily temperature increments and decrements, and this kind of symmetry can be quantified by distributions of consecutive daily mean temperature increasing or decreasing steps. At the same time, the findings above have been confirmed by artificially generated time series with given value of multiscale asymmetry.

1 Introduction

It has been defined that a stationary process $x(t)$ is time reversible if for every n the series $\{x_1, ..., x_n\}$ and $\{x_n, ..., x_1\}$ have the same joint probability distributions (Weiss 1975). This means this kind of process is invariant under the reversal arrow of time, and Gaussian linear processes belong to this kind of reversible processes. Conversely, time series irreversibility is believed to be indicative of the presence of nonlinearities in the underlying dynamics (Roldán and Parrondo 2010; Lacasa et al. 2012). Since nonlinearity results in an asymmetry of certain statistical properties under time reversal, studying temporal irreversibility of time series is taken to be an important indirect quantitative assessment of nonlinearity (Diks et al. 1995; Stone et al. 1996). To quantify the nonlinearity effect from the view point of time irreversibility has been applied to study observational time series from various fields of research such as physiological series (Yang et al. 2003; Costa et al. 2005; Cammarota and Rogora 2006; Costa et al. 2008; Donges et al. 2013).

Several statistical tests have been developed to detect and quantify irreversibility in time series (Daw et al. 2000; Cammarota and Rogora 2006; Costa et al. 2008; Lacasa et al. 2012; Donges et al. 2013). Most of these methods firstly perform a time series symbolization and usually make an empirical partition of the data range and then analyze the symbolized series by statistical comparison of symbol string occurrence in the forward and backward series (Daw et al. 2000). Due to an extra amount of ad hoc information for symbolization procedure, it has been thought that the results from these methods may depend on these extra parameters (Lacasa et al. 2012). Most recently, Lacasa and his colleges developed another method (Lacasa et al. 2012) based on horizontal visibility graph (Luque et al. 2009), which is an algorithmic variant of visibility graphs (Lacasa et al. 2008). Without an extra amount of ad hoc information for symbolization procedure, they show that irreversible dynamics results in an asymmetry between the probability distributions of the numbers of incoming and outgoing links in directed horizontal visibility graphs of given time series (Lacasa et al. 2012; Donges et al. 2013).

F. Xie · Z. Fu (✉) · L. Piao
Lab for Climate and Ocean-Atmosphere Studies, Department of Atmospheric and Oceanic Sciences, School of Physics, Peking University, Beijing 100871, China
e-mail: fuzt@pku.edu.cn

J. Mao
LASG, Institute of Atmospheric Physics, CAS, Beijing 100029, China

Since nonlinear processes govern the dynamics of many real-wold systems, temporal irreversibility may be an important property of many time series derived from processes in nature (Burykin et al. 2011). As one of the most important measures of natural changes, temperature records (Koscielny-Bunde et al. 1998; Bunde et al. 2005; Zhai and Pan 2003; Li et al. 2009; Yuan et al. 2010; Yuan and Fu 2014) are the best choice to carry on analysis of temporal irreversibility. Is there time-irreversible behavior in the daily mean temperature series? We will address this issue by the directed horizontal visibility graph (DHVG) method developed by Lacasa and his colleges (Lacasa et al. 2012). To our best knowledge, there is no answer in the literature to this issue. Though it has been found that there is a markedly nonlinear feature of daily terrestrial mean temperature, where the number of warming steps is significantly different from the number of cooing steps (Bartos and Jánosi 2005; Gyüre et al. 2007). There is also no answer whether this kind of local asymmetry found in daily mean temperature records is related to global temporal irreversibility; we will solve this problem from two aspects, observational analysis and calculations of deterministic time series with given asymmetric parameters.

The rest of the paper is organized as follows. In Section 2, we will make a brief introduction to the datasets used in this paper. We will focus on the DHVG method, the probability distributions of the steps of continuous increments or decrements, and the method quantifying the relationship between time irreversibility and asymmetry in Section 3. The results are discussed in Section 4. In Section 5, discussions and conclusions are made.

2 Data

In this article, daily mean temperatures from 182 stations are used for our analysis. The data are obtained from the China Meteorological Data sharing Service System (http://cdc.cma.gov.cn), with length of 53 years, from 1960 to 2012. Observations from all 182 meteorological stations are taken part in international exchange, and they have been homogenized (Li et al. 2009). Before our analysis, we first standardize the data by removing the seasonal trend through subtracting the annual cycle, as $T_i' = T_i - \langle T_i \rangle$ (Koscielny-Bunde et al. 1998), where T_i is the daily temperature and $\langle T_i \rangle$ is long-time climatological average for each calendar day. Just as has been accepted, this procedure cannot remove slow background trends such as a gradual shift of annual mean temperature (Bartos and Jánosi 2005).

In order to investigate nonlinear impact in original temperature anomaly variations, surrogate procedures such as shuffling (Makse et al. 1996; Govindan et al. 2007) have been applied to normalized temperature anomaly series to generate surrogated data with 1000 samples for each group. Fourier-filtering techniques can produce stochastic series which have the same power spectral density as the original series. However, for non-Gaussian distributions, the shape of probability density function (PDF) will not be preserved after Fourier filtering. In these cases, we applied an iterative algorithm introduced by Schreiber and Schmitz (1996) and Eichner et al. (2007) to keep the power spectral density and PDF unchanged. This is the so-called phase randomize surrogate procedure (PRS). These surrogated series will be analyzed and compared with original temperature anomaly series to investigate the effect of linear correlation and nonlinear correlations on asymmetrical behaviors. Meanwhile, a linear stochastic first-order autoregressive (AR(1)) process fitted to original temperature anomaly variations has been generated to check the nonlinear effect on asymmetrical behaviors. Since there are short memory and long-term memory in the mean daily temperature fluctuations, an improved version of AR(1), an extension of a first-order autoregressive model with power-law correlated noise, introduced by Király and his colleague (Király and Jánosi 2002), to simulate long-term memory and short-term memory in daily mean temperature fluctuations is adopted to generate surrogate series:

$$x_i = (\delta_1 - c)x_{i-1} + \varepsilon\eta_i, \tag{1}$$

where

$$c = 2(\alpha - 0.5)^{3/2} \tag{2}$$

$\delta_1 = 0.805$ and $\varepsilon = 2$ (as given by Király and colleagues), η_i is a long-term memory series which $\alpha = 0.63$.

Apart from above observational and surrogated series, a simple deterministic time series with exactly known properties (such as prescribed value of multiscale asymmetry) introduced by Burykin and his colleagues (Burykin et al. 2011) has been applied to generate determistic series for the sake of understanding the relation between temporal irreversibility and time asymmetry. They introduced an asymmetric Weierstrass function W_A (constructed from asymmetric sawtooth functions instead of cosine waves), and it is defined as follows:

$$W_A(t) = \sum_{k=1}^{k_{\max}} f_{\min}^{-kH} St(2\pi f_{\min}^{k} t + \varepsilon(k), \omega) \tag{3}$$

Here, $\omega (0 < \omega < 1)$ is an asymmetry parameter that determines the relative position of the maximum within one period of the sawtooth function $St(t)$, and $St(t)$ generates a sawtooth wave with period 2 for its argument t. H is the so-called Hurst exponent which is equal the detrended fluctuation analysis (DFA) exponent α. $\varepsilon(k)$ is a random series with uniform distribution within interval $(-\pi, \pi)$. Other parameters like $f_{\min}$ is the minimum frequency of oscillations and $k_{\max}$ is the maximum number of modes. And we

set $H = 0.67$ and different ω with range from 0 to 1 to generate 1000 group sequences for each w. Then we choose the length of each dataset $T_{\max} = 10$ s, the sampling frequency $f_s = 5000$ Hz, and the minimum frequency $f_{\min} = 1.5$ Hz.

3 Methods

3.1 DHVG

Following the works of Lacasa and his colleagues (Luque et al. 2009; Lacasa et al. 2012), we firstly transform each datum of a real-value time series $\{x_t\}_{t=1,\ldots,N}$ of N data points to a node in the horizontal visibility graph. And then links between two nodes i and j in the graph are calculated according to the following geometrical criterion (Lacasa et al. 2012; Luque et al. 2009; Donner et al. 2010):

$$x_n < x_i, x_j, \forall \quad n \quad |i < n < j \tag{4}$$

According to DHVG first introduced by Lacasa and his colleagues (Lacasa et al. 2012), the degree $k(t)$ of node t is now split into an ingoing degree $k_{\text{in}}(t)$, and an outgoing degree $k_{\text{out}}(t)$, such that $k(t) = k_{\text{in}}(t) + k_{\text{out}}(t)$. For a graphical illustration of the method, see Fig. 1. The in and out degree distributions of a DHVG are defined as the probability distributions of $k_{\text{out}}(t)$ and $k_{\text{in}}(t)$ of the graph, where

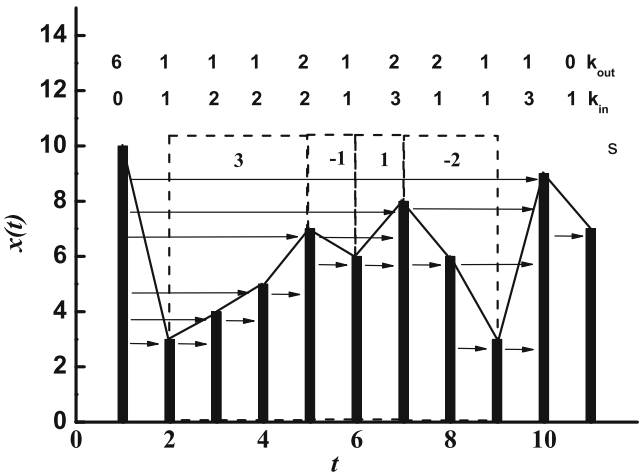

Fig. 1 Graphical illustration of DHVG and steps of consecutive increments and decrements. In the *bottom*, we plot a sample time series $\{x(t)\}$ with 11 data points. Each datum in the series is mapped to a node in the graph. *Arrows*, describing allowed directed visibility, link nodes. In this graph, each node has an ingoing degree k_{in}, which accounts for the numbers of links entering this node, and an outgoing degree k_{out}, for the numbers of links departing from this node; see the *top parts*. In the *middle parts*, *dash lines* outline the steps of consecutive increments and decrements, and s is step length of consecutive increments or decrements

$p_{\text{out}}(k) \equiv p(k_{\text{out}} = k)$ and $p_{\text{in}}(k) \equiv p(k_{\text{in}} = k)$. Lacasa and his colleagues (Lacasa et al. 2012) have proven

$$p_{\text{out}}(k) \equiv p_{\text{in}}(k) = \left(\frac{1}{2}\right)^k, \quad k = 1, 2, 3, \ldots \tag{5}$$

for uncorrelated stochastic series.

The DHVG method has not been applied to analyze the observational series, though it has been successfully applied to series from chaotic systems or generated stochastic series (Lacasa et al. 2012). In this paper, we will employ it to check the temporal irreversibility in observational temperature time series.

3.2 Steps of consecutive increments and decrements

Cooling rapidly and warming gradually asymmetry found in daily mean temperature records have been quantified by number differences between warming steps and cooling steps (Bartos and Jánosi 2005; Gyüre et al. 2007; Ashkenazy et al. 2008). In order to calculate steps of consecutive increments and decrements, symbolization procedure is applied to convert continuous valued time series measurements into a stream of discrete symbols. Typically, the range of the observed variable is partitioned into a finite number of bins, such that all measurements falling within a given bin are transformed into the same symbolic value. The objective in making such a transformation is to faithfully preserve dominant dynamical features while simplifying and speeding up subsequent computations. Let $\{x_t\}_{t=1,\ldots,N}$ be a real-value time series of N data points. We can classify a series into the two states: one is decreasing, the other is increasing. These two states are mapped to the symbols 0 and 1, respectively; see Fig. 1:

$$I_n = \begin{cases} 0, & \text{if} \quad x_n \leqslant x_{n-1} \\ 1, & \text{if} \quad x_n > x_{n-1} \end{cases} \tag{6}$$

We map the original series of length N to a binary sequence of length $N-1$ and calculate steps of consecutive symbols 0 (or 1). So s decreasing steps are defined as follows: for continuous time $[t, s+t+1]$, we have condition $x_t < x_{t+1} > x_{t+2} \ldots > x_{t+s} < x_{t+s+1}$. s increasing steps is defined as follows: we have condition $x_t > x_{t+1} \leqslant x_{t+2} \ldots \leqslant x_{t+s} > x_{t+s+1}$. And then probability distributions of s increasing or decreasing steps are $p_i(s) \equiv p(s_i = s)$ and $p_d(s) \equiv p(s_d = s)$. Let $\{x_t\}_{t=1,\ldots,\infty}$ be an infinite sequence of independent and identically distributed random variables extracted from a continuous probability density $f(x)$. Then, distributions of both consecutive decreasing and increasing steps are

$$p_d(s) \equiv p_i(s) = 3\left[\frac{1}{(s+1)!} - \frac{2}{(s+2)!} + \frac{1}{(s+3)!}\right]. \tag{7}$$

Next, we will give an explanation of the increasing states. For a given s, the probability is $\frac{\pi_s}{(s+3)!}$ in a stochastic series,

where π_s are the permutation of $x_t > x_{t+1} \leqslant x_{t+2} ... \leqslant x_{t+s+1} > x_{t+s+2}$. We can get $\pi_s = s^2 + 3s + 1$ and

$$p(s) \sim \frac{1}{(s+1)!} - \frac{2}{(s+2)!} + \frac{3}{(s+3)!}. \tag{8}$$

Using

$$\sum_{s=1}^{\infty} p(s) = 1, \tag{9}$$

we finally get

$$p_d(s) = p_i(s) = 3\left[\frac{1}{(s+1)!} - \frac{2}{(s+2)!} + \frac{1}{(s+3)!}\right]. \tag{10}$$

3.3 Quantifying time asymmetry and temporal irreversibility

We now study the information stored in the *in* and *out* distributions, taking into account the amount of temporal irreversibility and distributions of consecutive decreasing and increasing steps distributions taking into account the amount of time asymmetry of the associated series. And this can be measured as the distance (in a distributional sense) between the in and out degree distributions or the *decreasing* and *increasing* distributions. We make use of the absolute distance as the distance between two distributions. Given a random variable x and two probability distributions $p(x)$ and $q(x)$, absolute distance between p and q is defined as follows:

$$L(p,q) = \sum_{x\in\chi} |p(x)\log p(x) - q(x)\log q(x)|. \tag{11}$$

with $|10^{-m}\log 10^{-m}(m \to +\infty)| = 0\log 0 = 0$, where it is obvious that $L(p,q) = L(q,p)$, which vanishes if and only if both probability distributions are equal $p = q$ and it is bigger than zero otherwise. Why do we choose this measure to quantify the difference between two probability distributions $p(x)$ and $q(x)$, not other well defined measures? Two aspects let us make this choice. First, usually the maximum k_{out} (or s_d) is not equal to the maximum k_{in} (or s_i), and then we may meet the case $p(k_{\text{out}}) = 0$ (or $p(s_d) = 0$) but $p(k_{\text{in}}) \neq 0$ (or $p(s_i) \neq 0$) and vice versa, which will result in some singular points in some measures, but this will not occur in measure (11). Second, results from measure (11) is robust and will not qualitatively differ from results from other well-defined distance measures; we will show this in the last section.

The distance between $p_d(s)$ and $p_i(s)$ is

$$L_1(p_d, p_i) = \sum_s |p_d(s)\log p_d(s) - p_i(s)\log p_i(s)|, \tag{12}$$

while that between $p_{\text{in}}(k)$ and $p_{\text{out}}(k)$ is

$$L_2(p_{\text{in}}, p_{\text{out}}) = \sum_k |p_{\text{in}}(k)\log p_{\text{in}}(k) - p_{\text{out}}(k)\log p_{\text{out}}(k)|. \tag{13}$$

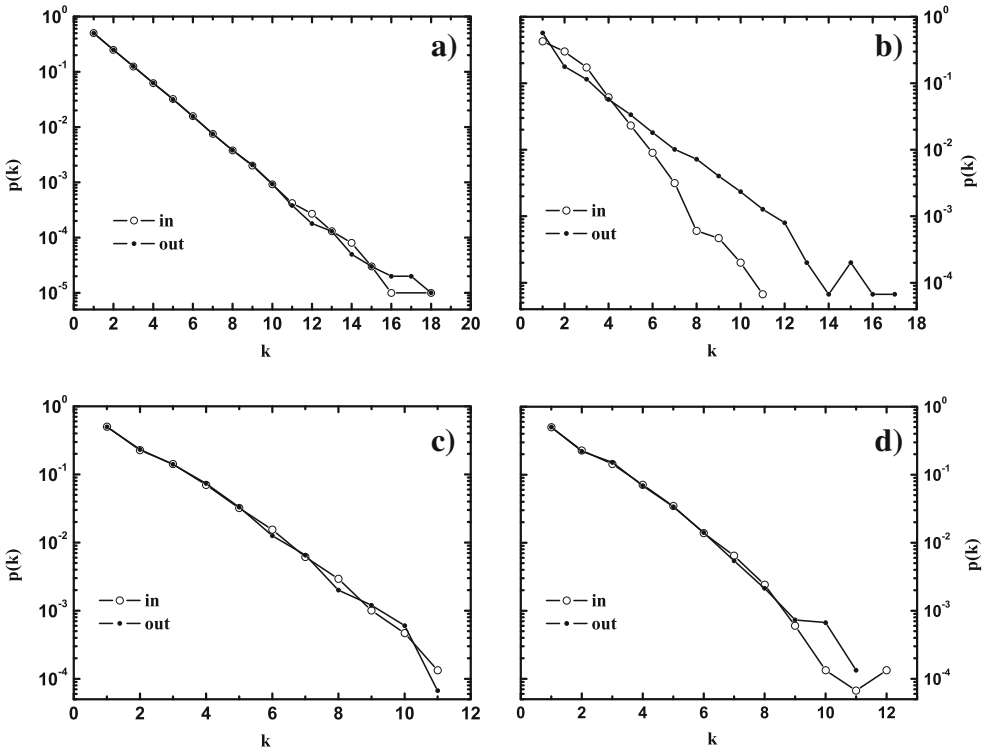

Fig. 2 The in and out degree distributions of DHVG associated to the **a** white noise series of 10^5 data points, **b** observational daily mean temperature anomaly series over Chongqing from 1960 to 2012, **c** AR(1) process fitted to the observational daily mean temperature anomaly series over Chongqing from 1960 to 2012, and **d** PRS generated series from the observational daily mean temperature anomaly series over Chongqing from 1960 to 2012. *Hollow circle* is p_{in} and *solid circle* is p_{out}

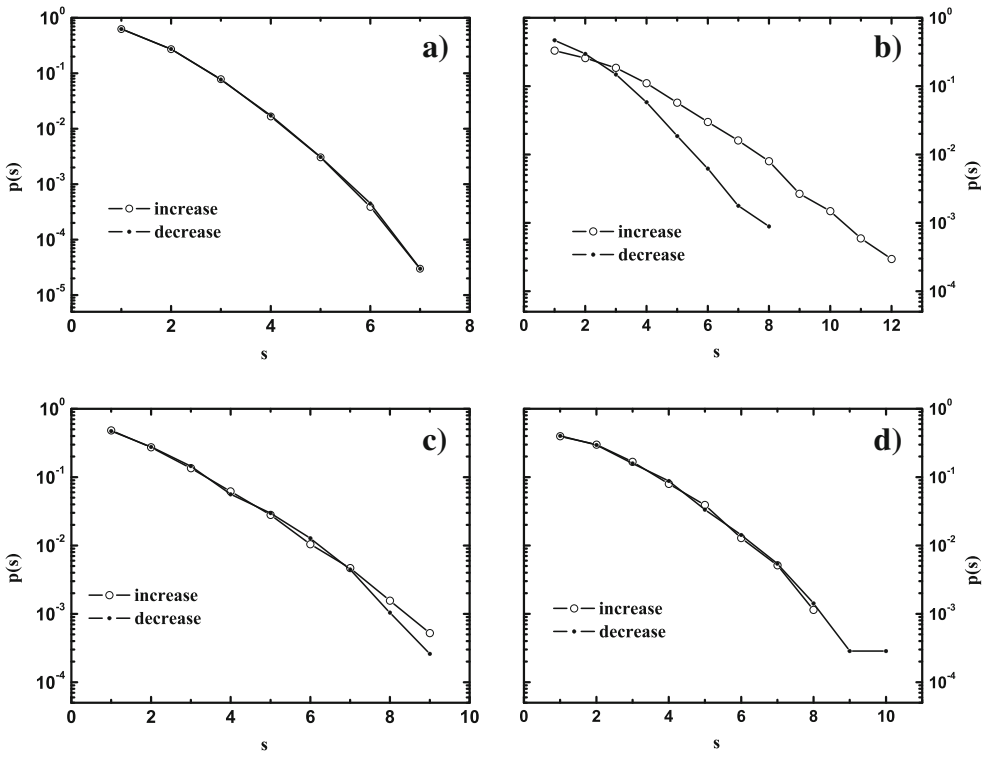

Fig. 3 The distributions of steps of consecutive increments and decrements associated to the **a** white noise series of 10^5 data points, **b** observational daily mean temperature anomaly series over Chongqing from 1960 to 2012, **c** AR(1) process fitted to the observational daily mean temperature anomaly series over Chongqing from 1960 to 2012, and **d** PRS generated series from the observational daily mean temperature anomaly series over Chongqing from 1960 to 2012. *Hollow circle* is p_i and *solid circle* is p_d

4 Results

4.1 Temporal irreversibility of temperature variations

First of all, the DHVG method is employed to daily mean temperature anomaly variations over a representative station, Chongqing (29° N, 106° E) situated at the transitional area between the Qinghai-Tibet Plateau and the plain on the middle and lower reaches of the Yangtze River in the subtropical climate zone often swept by moist monsoons. The DHVG results indicate that the difference between degree distributions of p_{in} and p_{out} over Chongqing is markedly predominant (see Fig. 2b), while this dominated difference cannot be found in linear processes, such as Gaussian white noise process (see Fig. 2a), where the degree distributions of p_{in} and p_{out} collapse toward a single line over a nearly whole range, the scatter over large k is caused by finite size of samples. Similar behaviors can be found in the AR(1) process (see Fig. 2c) and PRS surrogated series from original daily mean temperature anomaly variations over Chongqing (see Fig. 2d). Meanwhile, it is obvious that link length k is different for ingoing and outgoing link of daily mean temperature anomaly variations over Chongqing, the maximum k_{out} is 17, while the maximum k_{in} is only 11. However, the lengths of ingoing and outgoing link for Gaussian white noise process are equal, AR(1) and PRS surrogated processes. All these results suggest that the daily mean temperature anomaly variations over Chongqing is a time-irreversible process, and quantitative measure of time irreversibility given by L_2 is $L_2(p_{\text{out}}, p_{\text{in}}) = 0.328$.

What causes this markedly global time irreversibility in daily mean temperature anomaly variations over Chongqing? One possible mechanism is the time asymmetry found in the local trend in daily mean temperature anomaly variations over mid-latitudes (Ashkenazy et al. 2008). This kind of time asymmetry can be quantified by steps of consecutive increments and decrements of temperature variations; see Fig. 3. Figure 3b shows that the distribution of steps of consecutive increments s_i departs from that for steps of consecutive increments s_d in the observational records. However, this feature cannot be found in the linear processes, such as Gaussian white noise process given in Fig. 3a, AR(1) process fitted to the observational records shown in Fig. 3c, and PRS surrogated series in Fig. 3d. We can also find that the maximum length of consecutive increments and decrements of temperature variations is

Table 1 L_1 and L_2 calculated from observational series, AR(1) fitted to the same observational series, PRS generated series from the same observational series, and from Gaussian white noise series

	Obs.	AR(1)	PRS	White noise
L_1	0.328	0.0126	0.0125	0.00249
L_2	0.412	0.0177	0.0201	0.00281

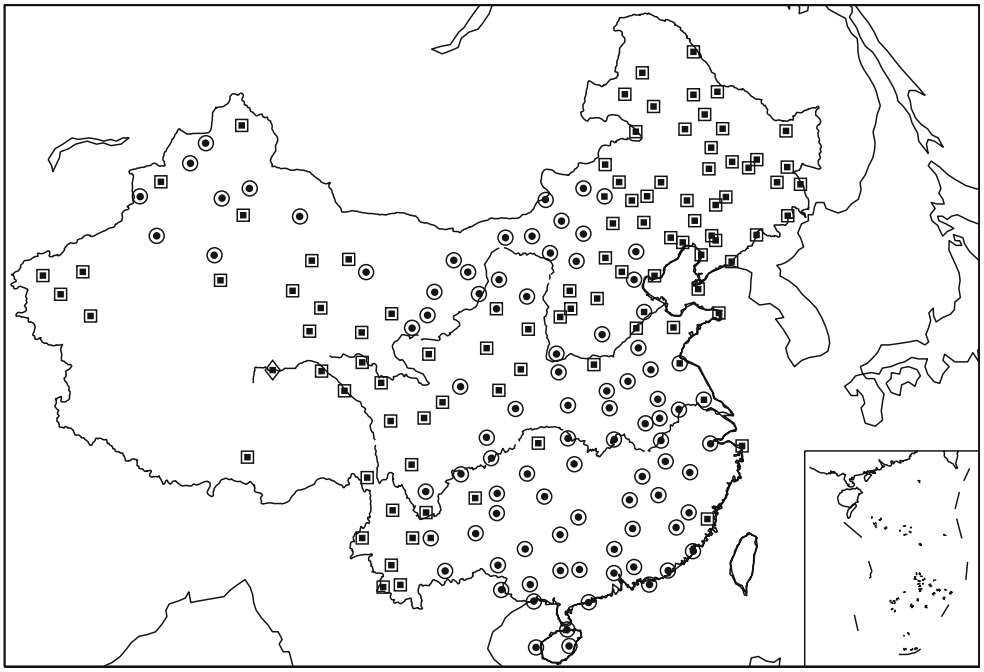

Fig. 4 Spatial distributions of L_1 and L_2. *Hollowed symbols* for L_2 and *solid symbols* for L_1. The *circles* denote $\bar{L}_i < L_i$, $(i = 1, 2)$, *squares* denote $L_{ic} < L_i \leq \bar{L}_i$, $(i = 1, 2)$, and *rhombuses* denote $L_i \leq L_{ic}$, $(i = 1, 2)$

different; there are longer length for consecutive increments (11) than decrements (8), i.e., cooling quickly and warming gradually will be often found in the temperature variations. The quantified difference is $L_1 = L(p_i, p_d) = 0.412$. The better concordance between L_1 and L_2 is revealed in Table 1 for comparison between results in Figs. 2 and 3. Compared to the linear processes, AR(1) or PRS surrogated processes, the value of L_1 or L_2 from observational series is one order larger, even two orders larger than those from Gaussian white noise processes.

Apart from these results, Fig. 4 displays the better spatial concordance between L_1 and L_2 over whole

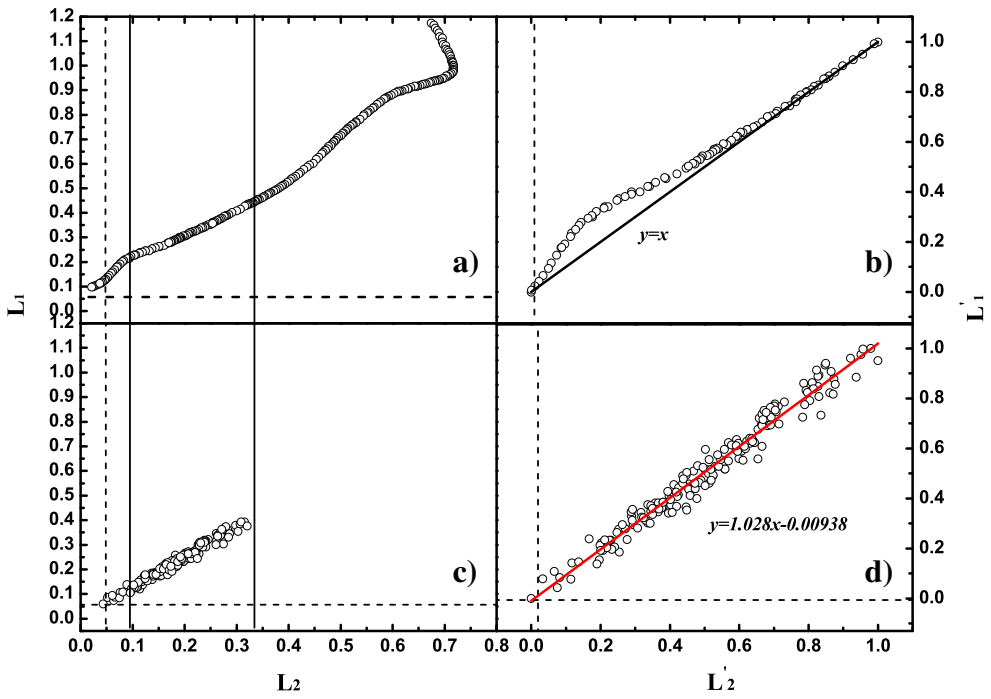

Fig. 5 The scatter plots of L_1 vs L_2 and L_1' vs L_2'. **a**, **b** Theoretical series with $H = 0.67$; **c**, **d** observational daily mean temperature anomaly series over 182 stations from 1960 to 2012. Here, the *horizontal* and *vertical dash lines* denote statistically significant time series irreversibility when L_1 and L_2 are above or right over these lines

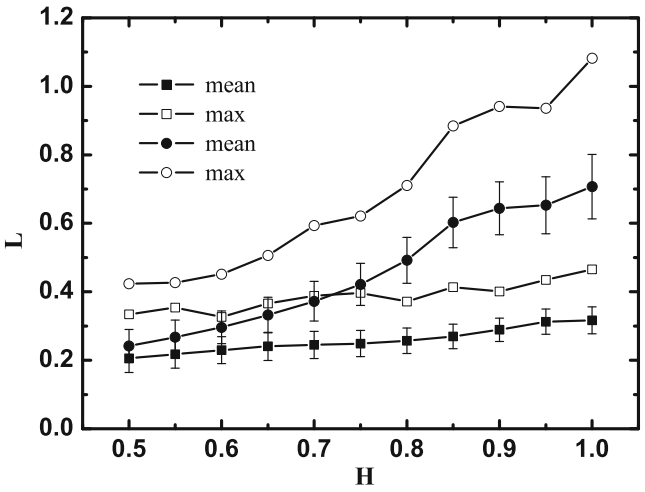

Fig. 6 Variations of L_1 and L_2 with different H and $\omega = 0.066$ calculated from 1000 samples. *Hollow circles* for maximal L_1 and *solid circles* for mean L_1 with one standard deviation. *Hollow squares* for maximal L_2 and *solid squares* for mean L_2 with one standard deviation

regions of China. The largest time series irreversibility or temporal asymmetry simultaneously can be found over south of China, and larger time series irreversibility or temporal asymmetry simultaneously occurs over northeast and southwest of China. Although we adopt different measures, this spatial distribution of time series irreversibility or temporal asymmetry recovers the results given in Ashkenazy et al. (2008), where NCEP reanalysis temperature records have been applied to study surface daily mean temperature cooling rapidly and warming gradually at the mid-latitudes. This great concordance between L_1 and L_2 can also be found in their scatter plots in Fig. 5c, d, where Fig. 5c is result for L_1 and L_2 from observational records over 182 stations, while Fig. 5d is for re-scaled L_1 and L_2 by $L_i' = \frac{L_i - \min(L_i)}{\max(L_i) - \min(L_i)}, i = 1, 2$. It is obvious there is great linear correspondence between L_1 and L_2 over the whole range.

4.2 Results from deterministic time series

Analysis for the observational records suggests there is great well concordance between qualifier L_1 and L_2. Could this concordance be justified in theoretical records? Over the range (the values that L_2 takes) the same as observational records, similar linear concordance between L_1 and L_2 is found for theoretical records, only when L_2 takes smaller value in a narrower range, i.e., $L_2 < 0.15$, there is a little depart from the linear behavior; see Figs. 5a, b, where H is set to be 0.67, the same as the mean value calculated from the observational daily mean temperature variations (Yuan et al. 2010). Actually, it can be found that over the whole range that L_2 could cover, linear feature between L_1 and L_2 can be found only in some intervals (see Fig. 5a), and there are some transition points. The reason causing this feature is that there are two parameters to control the variations for the theoretical time irreversibility process, i.e., H and ω. And these two parameters affect two qualifiers differently. L_1 is much sensitive to the variation of H, but L_2 is not, which can be found in Fig. 6. This results from that L_2 quantifies the time series irreversibility, which is not affected by memory intensity of associated processes, and L_1 quantifies intensity of the local asymmetrical variations of associated processes, which can be affected by the memory intensity of associated processes, since there will be more large-scale structures in the stronger long-range correlated processes. Over the weak range of asymmetry parameter ω, both L_1 and L_2 change nearly linearly with variation of ω, and only L_1 has some weakly jumping points; see Fig. 7a. With the asymmetry intensity increasing (the value of ω decreases), both L_1 and L_2 dramatically depart from their linear variation with ω. And the ratio between L_1 and L_2 provides a vivid feature for these variations (see Fig. 7b), where there are two dominated linear ranges over the middle parts of asymmetry intervals. Surprisingly, both L_1 and L_2 calculated from daily mean anomaly temperature variations over all stations in China are within these two linear ranges; see Figs. 5c and 7.

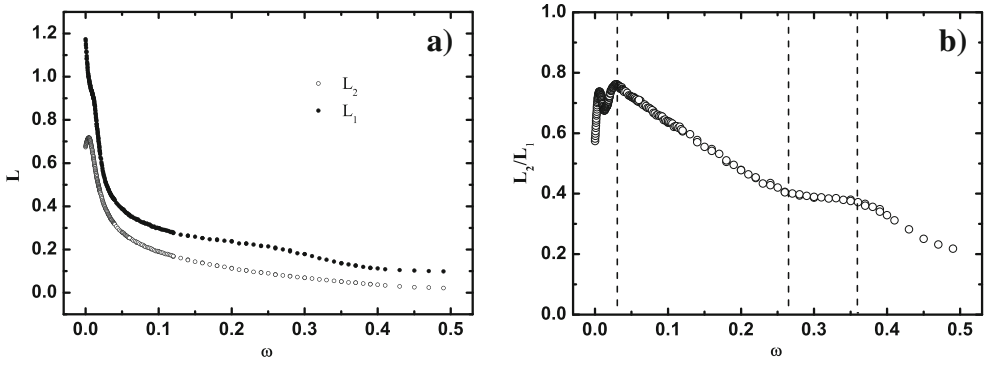

Fig. 7 **a** Variations of L_1 and L_2 with different ω and $H = 0.67$. **b** Variations of L_2/L_1 with different ω and $H = 0.67$

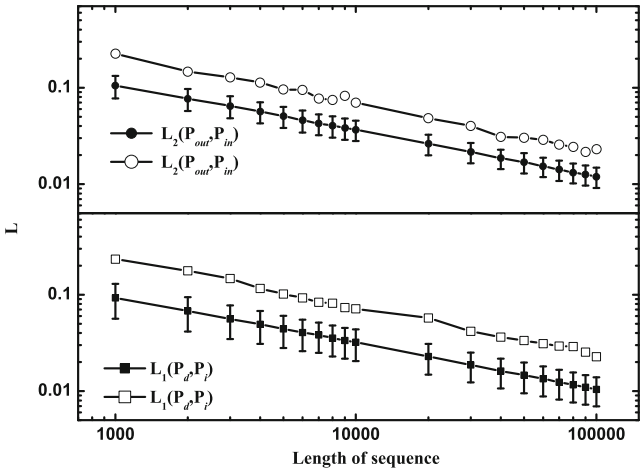

Fig. 8 Variations of L_1 and L_2 with different series length calculated from white noise series

5 Conclusion and discussion

To determine whether daily mean anomaly temperature variations are irreversible or not, a criteria is required to test its statistical significance. We calculate $L_1(p_i, p_d)$ and $L_2(p_{\text{in}}, p_{\text{out}})$ for Gaussian noise of different lengths (from 10^3 to 10^5), as shown in Fig. 8, and we can conclude that both mean and maximum values of L_1 and L_2 decrease with increasing series length. To reach a reliable numerical statistics, there are 1000 samples in each group with the same length. Detailed statistics for L_1 and L_2 have been listed in Table 2, where the mean value, standard deviation, and maximum of L_1 and L_2 have been provided. The criteria to define a piece of time series with given length to be time series irreversible here is to set the maximum $L_2(p_{\text{in}}, p_{\text{out}})$ and $L_1(p_i, p_d)$ in the 1000 simulations as the lowest boundary for time series irreversibility. For series of length 2×10^4, nearly equal to the series length of observational temperature variations used in this paper, the critical value for L_{1c} is 0.0572 and L_{2c} is 0.0481, which have been plotted as the horizontal and vertical dash lines in Fig. 5 to denote as statistically significant time series irreversibility when L_1 and L_2 are above or right over these lines. Obviously, daily mean anomaly temperature variations over all but one stations are significantly (confidence level >99.99 %) time series irreversible.

The above results show that statistics calculated from DHVG and steps of consecutive increments and decrements over certain ranges can be employed to give the same quantified measure on time series irreversibility or temporal asymmetry. Actually, DHVG describe the global links between different nodes, especially for those nodes of extreme values; however, steps of consecutive increments and decrements quantify mainly the local interactions. If the asymmetry intensity of associated processes is not so large, quantifiers from both DHVG and steps of consecutive increments and decrements will give the same results. Since calculation of steps of consecutive increments and decrements is much simpler than that for DHVG, in some cases, we can choose calculation of steps of consecutive increments and decrements to quantify time series irreversibility of associated processes.

All the above results are calculated from measure (11); are they robust to other well-defined measures? We will answer this question next. Here, we compare results from measure (11) to those from other two well-defined measures: the Kullback-Leibler divergence (Cover and Thomas 2006; Kowalski et al. 2011) used by Lacasa et al. (2012) and Euler distance between distributions (Cover and Thomas 2006; Kowalski et al. 2011).

The Kullback-Leibler divergence (Lacasa et al. 2012; Cover and Thomas 2006; Kowalski et al. 2011) is defined as

$$D(p(x)\|q(x)) = \sum_{x\in\chi} p(x)\log\frac{p(x)}{q(x)}. \tag{14}$$

where $D(p(x)\|q(x)) \neq D(q(x)\|p(x))$ in general and we use the convention that $0\log\frac{0}{0} = 0$, $0\log\frac{0}{q} = 0$ and $p\log\frac{p}{0} = \infty$ (Cover and Thomas 2006). However, in our calculation of $D(p(x)\|q(x))$ from the observational series, $p = 0$ or $q = 0$ only occurs when the value of links k or steps s is larger, but its probability is much smaller (see Figs. 2b and 3b), in order to avoid that this case ($p\log\frac{p}{0} = \infty$) determines the calculation of $D(p(x)\|q(x))$, we take $p\log\frac{p}{0} = 0$. This is also why we do not choose

$D(p(x)\|q(x))$

as a major measure in our works.

Table 2 Statistics of L_1 and L_2 calculated Gaussian white noise series of different length sizes

Length (10^3)	0.5	1	2	4	8	10	20	100
$\bar{L_2}$	0.144	0.105	0.0771	0.0566	0.0405	0.0368	0.0262	0.0120
$\max(L_2)$	0.306	0.226	0.147	0.113	0.0748	0.0700	0.0481	0.0230
$\sigma(L_2)$	0.0404	0.0275	0.0199	0.0140	0.0100	0.00884	0.00624	0.00285
$\bar{L_1}$	0.129	0.0928	0.0677	0.0493	0.0354	0.0321	0.0229	0.0104
$\max(L_1)$	0.345	0.233	0.177	0.116	0.0813	0.0712	0.0572	0.0227
$\sigma(L_1)$	0.0518	0.0365	0.0262	0.0184	0.0125	0.0116	0.00804	0.00347

And then the Kullback-Leibler divergence between $p_d(s)$ and $p_i(s)$ is

$$D_1(p_d \| p_i) = \sum_s p_d(s) \log \frac{p_d(s)}{p_i(s)}, \tag{15}$$

while Kullback-Leibler divergence between $p_{\text{in}}(k)$ and $p_{\text{out}}(k)$ is

$$D_2(p_{\text{in}} \| p_{\text{out}}) = \sum_k p_{\text{in}}(k) \log \frac{p_{\text{in}}(k)}{p_{\text{out}}(k)}. \tag{16}$$

The Euler distance between distributions (Cover and Thomas 2006; Kowalski et al. 2011) is defined as

$$E(p(x), q(x)) = \sum_{x \in \chi} |p(x) - q(x)|. \tag{17}$$

where it is obvious $E(p(x), q(x)) = E(q(x), p(x))$.

And then the distance between $p_d(s)$ and $p_i(s)$ is

$$E_1(p_d, p_i) = \sum_s |p_d(s) - p_i(s)|, \tag{18}$$

while distance between $p_{\text{in}}(k)$ and $p_{\text{out}}(k)$ is

$$E_2(p_{\text{in}}, p_{\text{out}}) = \sum_k |p_{\text{in}}(k) - p_{\text{out}}(k)|. \tag{19}$$

Actually, the results are robust and not sensitive to the measure we have chosen; see Fig. 9. It is obvious that both the Kullback-Leibler divergence and Euler distance reach the similar conclusion as we have shown from measure (11). Nearly all the temperature variations over China are time asymmetric and temporal irreversible. And the results from both the horizontal visibility graph and consecutive steps of increase or decrease variations are linearly dependent each other. Due to this, here we only present comparisons between measure (12) with measures 15 and 18 (see Figs. 9c, d), where both measures give qualitatively the same results, although the Euler distance seems a little scattering.

At last, we want to point out that fluctuations of many atmospheric variables are considered to be well approximated by low-order autoregressive (AR) processes on small time scales (von Storch and Zwiers 1999). An AR model describing a fluctuating signal as a linear function of its past values plus an uncorrelated noise term is taken to be fully adequate and there seems to be a consensus in the literature for daily surface temperature records that higher than the second-order AR models are rarely needed after proper detrending (Bartos and Jánosi 2005). However, the results shown in this paper indicate that the linear processes cannot capture the nonlinear features hidden in the measured series. Since nearly all daily mean temperature anomaly series are time series irreversible or temporal asymmetry, in order to properly describe the nonlinear features of daily mean temperature anomaly variations, new statistical model is required. Since it has been found that cooling rapidly and warming gradually asymmetry found in daily mean temperature records over mid-latitudes is partially related to cold fronts (Ashkenazy et al. 2008), where nonlinear behavior

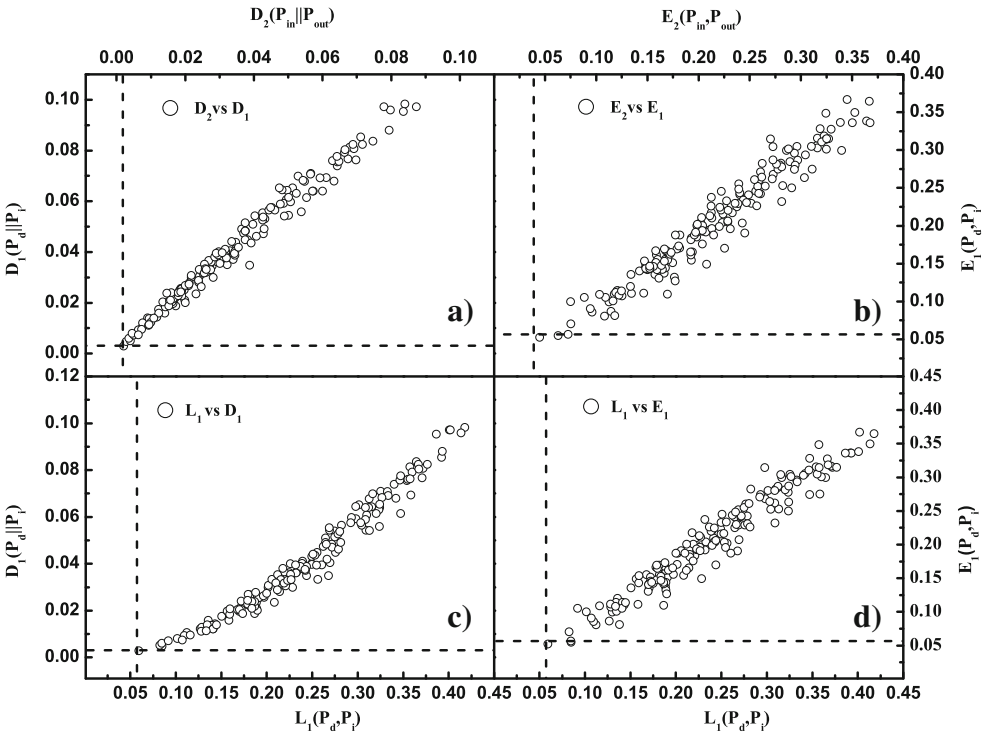

Fig. 9 The scatter plots of **a** D_1 vs D_2, **b** E_1 vs E_2, **c** L_1 vs D_1, and **d** L_1 vs E_1 from the observational daily mean temperature anomaly series over 182 stations from 1960 to 2012. Here, the *horizontal* and *vertical dash lines* denote statistically significant time series irreversibility when calculated measures are above or right over these lines

is more important, incorporating nonlinearity to understand and correctly model this kind of time asymmetry or temporal irreversibility is of great importance to reproduce physical system in more details and to explain fundamental dynamics from a higher-order approximation.

Acknowledgments Many thanks are due to valuable suggestions from two anonymous reviewers and supports from the National Basic Research Programme of China (Nos. 2014CB953902 and 2011CB403505) and National Natural Science Foundation of China (Nos. 41175141 and 41475048).

References

Ashkenazy Y, Feliks Y, Gildor H, Tziperman E (2008) Asymmetry of daily temperature records. J. Atmos. Sci. 65:3327

Bunde A, Eichner JF, Kantelhardt JW, Havlin S (2005) Long-term memory: a natural mechanism for the clustering of extreme events and anomalous residual times in climate records. Phys Rev Lett 94:048701

Bartos I, Jánosi IM (2005) Atmospheric response function over land: strong asymmetries in daily temperature fluctuations. Geophys Res Lett 32:L23820

Burykin A, Costa M, Peng CK, Goldberger AL, Buchman TG (2011) Generating signals with multiscale time irreversibility: the asymmetric weierstrass function. Complexity 16:29

Cammarota C, Rogora E (2006) Time reversal, symbolic series and irreversibility of human heartbeat. Chao, Solitons & Fractals 32:1649–1654

Costa M, Goldberger AL, Peng CK (2005) Broken asymmetry of the human heartbeat: loss of time irreversibility in aging and disease. Phys Rev Lett 95:198102

Costa M, Peng CK, Goldberger AL (2008) Multiscale analysis of heart rate dynamics: entropy and time irreversibility measures Cardiovasc Eng. doi:10.1007/s10558-007-9049-1

Cover TM, Thomas JA (2006) Elements of information theory. Wiley, New Jersey

Daw CS, Finney CEA, Kennel MB (2000) Symbolic approach for measuring temporal irrevetsibility. Phys Rev E 62:1912–1921

Diks C, van Houwelingen JC, Takens F, DeGoede J (1995) Reversibility as a criterion for discriminating time series. Phys Lett A 201:221–228

Donner RV, Zou Y, Donges JF, Marwan N, Kurths J (2010) Recurrence networks: a novel paradigm for nonlinear time series analysis. New J Phys 12:033025

Eichner JF, Kantelhardt JW, Bunde A, Havlin S (2007) Statistics of return intervals in long-term correlated records. Phys Rev E 75:011128

Govindan RB, Wilson JD, Preißl H, Eswaran H, Campbell JQ, Lowery CL (2007) Detrended fluctuation analysis of short datasets: an application to fetal cardiac data. Physica D 226:23

Gyüre B, Bartos I, Jánosi IM (2007) Nonlinear statistics of daily temperature fluctuations reproduced in a laboratory experiment. Phys Rev E 76:037301

Donges JF, Donner RV, Kurths J (2013) Testing time series irreversibility using complex network methods. EPL 102:10004

Király A, Jánosi IM (2002) Stochastic modeling of daily temperature fluctuations. Phys Rev E 65:051102

Koscielny-Bunde E, Bunde A, Havlin S, Roman HE (1998) Indication of a universal persistence law governing atmospheric variability. Phys Rev Lett 81:729

Kowalski AM, Martin MT, Plastino A, Rosso OA, Casas M (2011) Distances in probability space and the statistical complexity setup. Entropy 13:1055–1075

Lacasa L, Nuñez A, Roldan E, Parrondo JMR, Luque B (2012) Time series irreversibility: a visibility graph approach. Eur Phys J B 85:217

Li Q, Zhang H, Chen J, Li W, Liu X, Jones P (2009) A mainland China homogenized historical temperature dataset for 1951∼2004. Bull Amer Meteor 90:1062

Lacasa L, Luque B, Ballesteros F, Luque J, Nuño JC (2008) From time series to complex networks: the visibility graph. Proc Natl Acad Sci 105:4972–4975

Luque B, Lacasa L, Ballesteros F, Luque J (2009) Horizontal visibility graphs: exact results for random time series. Phys Rev E 80:046103

Makse HA, Havlin S, Schwartz M, Stanley HE (1996) Method for generating long-range correlations for large systems. Phys Rev E 53:5445

Roldán E, Parrondo JMR (2010) Estimating dissipation from single stationary trajectories. Phys Rev Lett 105:15

Schreiber T, Schmitz A (1996) Improved surrogate data for nonlinearity tests. Phys Rev Lett 77:635–638

Stone L, Landan G, May RM (1996) Detecting time's arrow: a method for identifying nonlinearity and deterministic chaos in time-series data. Proc R Soc Lond B 263:1509–1513

von Storch H, Zwiers FW (1999) Statistical analysis in climate research. Cambridge University Press, Cambridge

Weiss G (1975) Time-reversibility of linear stochastic processes. J Appl Prob 12:831–836

Yang ACC, Huseu SS, Yien HW, Goldberger AL, Peng CK (2003) Linguistic analysis of the human heartbeat using frequency and rank order statistics. Phys Rev Lett 90:108103

Yuan NM, Fu ZT, Mao JY (2010) Different scaling behaviors in daily temperature records over China. Physica A 389:4087

Yuan NM, Fu ZT (2014) Century-scale intensity modulation of large-scale variability in long historical temperature records. J Climate 27:1742

Zhai PM, Pan XL (2003) Trends in temperature extremes during 1951∼1999 in China. Geophys Res Lett 30:1913